DTIC FILE COPY

(2)

HDL-TM-90-13

AD-A226 685

August 1990

Effect of Laser Fluctuations in Automated Solder Joint Inspection

by Andrew J. Bayba

DTIC
ELECTE
SEP 25 1990
S B D

U.S. Army Laboratory Command
Harry Diamond Laboratories
Adelphi, MD 20783-1197

Approved for public release; distribution unlimited.

90 09 20 069

The findings in this report are not to be construed as an official Department of the Army position unless so designated by other authorized documents.

Citation of manufacturer's or trade names does not constitute an official endorsement or approval of the use thereof.

Destroy this report when it is no longer needed. Do not return it to the originator.

UNCLASSIFIED

SECURITY CLASSIFICATION OF THIS PAGE

REPORT DOCUMENTATION PAGE

Form Approved
OMB No. 0704-0188

1a. REPORT SECURITY CLASSIFICATION Unclassified	1b. RESTRICTIVE MARKINGS
2a. SECURITY CLASSIFICATION AUTHORITY	3. DISTRIBUTION/AVAILABILITY OF REPORT Approved for public release; distribution unlimited.
2b. DECLASSIFICATION/DOWNGRADING SCHEDULE	
4. PERFORMING ORGANIZATION REPORT NUMBER(S) HDL-TM-90-13	5. MONITORING ORGANIZATION REPORT NUMBER(S)
6a. NAME OF PERFORMING ORGANIZATION Harry Diamond Laboratories 6b. OFFICE SYMBOL (if applicable) SLCHD-TS-PT	7a. NAME OF MONITORING ORGANIZATION
6c. ADDRESS (City, State, and ZIP Code) 2800 Powder Mill Road Adelphi, MD 20783-1197	7b. ADDRESS (City, State, and ZIP Code)
8a. NAME OF FUNDING/SPONSORING ORGANIZATION U.S. Army Material Command 7b. OFFICE SYMBOL (if applicable)	9. PROCUREMENT INSTRUMENT IDENTIFICATION NUMBER
8c. ADDRESS (City, State, and ZIP Code) 5001 Eisenhower Avenue Alexandria, VA 22333	10. SOURCE OF FUNDING NUMBERS PROGRAM ELEMENT NO. P78011 PROJECT NO. DE50 TASK NO. WORK UNIT ACCESSION NO.

11. TITLE (Include Security Classification)
Effect of Laser Fluctuations in Automated Solder Joint Inspection

12. PERSONAL AUTHOR(S)
Andrew J. Bayba

13a. TYPE OF REPORT	13b. TIME COVERED	14. DATE OF REPORT (Year, Month, Day)	15. PAGE COUNT
Final	FROM Sep 89 TO Mar 90	August 1990	17

16. SUPPLEMENTARY NOTATION
AMS code: 768016E50; HDL Project No: 8E0087

17. COSATI CODES		
FIELD	GROUP	SUB-GROUP
09	01	
14	02	

18. SUBJECT TERMS (Continue on reverse if necessary and identify by block number)
Thermal signature, solder joint inspection, inspection using lasers

19. ABSTRACT (Continue on reverse if necessary and identify by block number)

A study was performed to assess the significance of potential fluctuations in power output of the heating laser in automated laser inspection systems. So that the effect of variations in power output could be determined, heat-transfer analysis was conducted on a simplified model of a solder connection using finite-element methods. The study indicates that 10-percent modulation about some mean power input produces the same frequency of modulation as the input, but slightly damped amplitude, in the infrared emissions measured during the heat-up phase; the error is negligible after the laser is terminated. The study also indicates that a 10-percent increase or decrease in average power input produces an error in measured infrared emissions of approximately 11 percent throughout the process. The latter results were corroborated by a mathematical model.

20. DISTRIBUTION/AVAILABILITY OF ABSTRACT ☒ UNCLASSIFIED/UNLIMITED ☐ SAME AS RPT. ☐ DTIC USERS	21. ABSTRACT SECURITY CLASSIFICATION Unclassified
22a. NAME OF RESPONSIBLE INDIVIDUAL Andrew J. Bayba	22b. TELEPHONE (Include Area Code) (202) 394-4340 22c. OFFICE SYMBOL SLCHD-TS-PT

DD Form 1473, JUN 86 Previous editions are obsolete. SECURITY CLASSIFICATION OF THIS PAGE

UNCLASSIFIED

Contents

Page

1. Introduction 5
2. Machine Description 6
3. Analysis Procedure 7
4. Results 8
5. Conclusions 14

Distribution 15

Figures

1. Typical power versus time plot of laser output 6
2. Laser power input for finite-element analysis load cases 8
3. Finite-element analysis temperature plots for sinusoidal and normal power pulses 9
4. Temperature plots for increased, decreased, and normal power pulses 9
5. Infrared emission for sinusoidal and normal power pulses 11
6. Infrared emission for increased, decreased, and normal power pulses 11
7. Percentage difference in infrared emissions from normal power pulse 12

Table 1. Error predictions of IR emissions 13

DTIC COPY INSPECTED

Accession For
NTIS GRA&I ☑
DTIC TAB ☐
Unannounced ☐
Justification
By
Distribution/
Availability Codes
Dist | Avail and/or Special
A-1

1. Introduction

Laser inspection of solder connections is a state-of-the-art technology that determines the acceptability of a soldered connection by comparing the thermal signature (the heat-up and cool-down curves) of the connection with the thermal signature of a known good connection. The theory is that a defect in the connection, such as a detached lead, will alter the connection's thermal properties so that its thermal signature will be identifiably different from that of the good connection. Thermal signatures are acquired by irradiating the connection with a laser for a given period of time while monitoring the heat radiated from the object with an infrared detector.

The Department of Defense (DoD) is interested in this technology because of its possible application to the assessment of certain key properties of leads and connections, such as solderability, surface cleanliness, and bulk volume. The rate per unit area at which energy is radiated from an object is determined by only two basic variables: emissivity and surface temperature. However, these two variables depend on several other factors. The emissivity is primarily dependent on the material being considered and its surface condition, while the surface temperature depends on heat-transfer conditions, such as input energy, object volume, and thermal properties of the material. DoD believes that it may be possible to characterize the shape of the thermal signatures, thus allowing for the isolation of anomalies in certain of the properties just discussed. If this is the case, this technology could be used in a variety of areas of concern in electronics process control.

Since the radiant heat measured by the machine depends on the input energy from the heating source, the accuracy of the measurements would be suspect if the stability of the heating source output was in question. The possibility of error introduced by the heating source began to be considered when it was noted that the power output of the laser currently used in this technology has shown substantial modulation during the heating phase (see fig. 1).

Two possibilities for error are apparent. First, the sinusoidal-type modulation may have some transient effect on the temperature at the surface, where the infrared emission is measured. Second, severe fluctuations might give a net power input increase or decrease, producing some unknown deviation in the infrared emission measured. Both possibilities were analyzed using finite-element analysis, the second in two parts to account for both an increase and a decrease.

The first case was modeled by producing a sinusoidal input about a mean value, and the other two cases were modeled by producing flat

inputs 10 percent above and below the same mean value. The resulting infrared emissions were then compared to those produced when the mean value is used as an input. The purpose of this analysis is not to give exact results, but to provide information on trends in percentage of error of the IR radiation readings caused by power variations of these types.

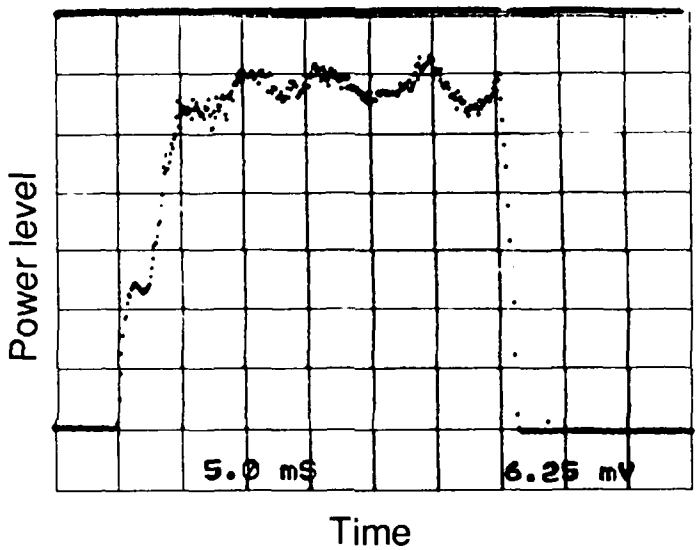

Figure 1. Typical power versus time plot of laser output.

2. Machine Description

The Vanzetti LI/6000 Laser/Inspect is an instrument which employs the technology described previously. The machine inspects objects in a closed environment at room temperature. The heat source is a 30-W yttrium aluminum garnet (YAG) laser emitting in the infrared at a 1.06-μm wavelength. The laser delivers a maximum of 18 to 22 W of useful energy to the surface of the object, after transmission through the machine's optic system. However, the laser power is adjustable, and a setting of 16 W of delivered power is standard for solder joint assessment. The power absorbed by the object, which is somewhat less than this, is determined by the absorptance of the material. The laser is focused onto a spot 0.43 mm in diameter and typically held for between 10 and 100 ms, depending on the volume and type of specimens under investigation. The infrared emission produced by the object is measured with an InSb photovoltaic infrared detector. The area from which the infrared emission is gathered is the same as that which is irradiated by the laser.

3. Analysis Procedure

The sample object analyzed in this report is the solder cylinder formed in a plated-through-hole connection. This study neglects the possible effects of a lead, the component heat sink, the copper plating, etc, so that the general effect of fluctuations in input power is more readily apparent without complicating the heat flow. It is assumed that the percentage of deviation in infrared emissions from this simple case will be indicative of the kinds of deviations that might be found in more complicated cases.

Finite-element analysis was used to perform the heat-transfer analysis. The solder sample was modeled as a cylinder 1.95 mm deep with a diameter of 1 mm. The sides of the cylinder were modeled as fully insulated, since the boundary is epoxy; the top and bottom, being exposed to the environment, were given radiative boundary conditions. The inspection chamber was closed to outside airflow, so that loss by convective heat transfer was due only to natural convection. Film coefficients, $\bar{h}$, for the top and bottom of the cylinder were found to be 19.16 and 9.58 $Wm^{-2}K^{-1}$, respectively, by applying the following equation:

$$\bar{h} = \overline{N_u}\frac{K}{L}, \tag{1}$$

where $\overline{N_u}$ is the mean Nusselt number, K is the thermal conductivity, and L is the characteristic length.[1] The initial temperature of the solder and the ambient temperature of the environment were given as room temperature, 298 K. The ambient temperature was made to remain constant during the analysis, assuming the environment to be infinite compared to the sample size. Properties of the solder were as follows:[2,3]

$$\begin{aligned} \text{emissivity, } \varepsilon, &= 0.057, \\ \text{density, } \rho, &= 8500\ \text{kgm}^{-3}, \\ \text{thermal conductivity, } K, &= 50\ \text{Jm}^{-2}\text{s}^{-1}\text{K}^{-1}, \\ \text{specific heat, } C, &= 176\ \text{Jkg}^{-1}\text{K}^{-1}, \\ \text{absorptivity, } \alpha, &= 0.107. \end{aligned}$$

Four load cases were analyzed, shown in figure 2. A value of 1.712 W was chosen to be the normal power input, found by multiplying 16 W by the absorptivity. The sinusoidal input was given a peak-to-peak variation of 20 percent from the normal power value and a frequency

[1] *L. C. Thomas, Fundamentals of Heat Transfer, Prentice-Hall, Inc., Englewood Cliffs, NJ (1980), pp 437–445.*
[2] *M. P. Seah and C. Lea, Certainty of Measurement Using an Automated Infrared Laser Inspection Instrument for PCB Solder Joint Integrity, J. Phys. E (Scientific Instruments), 18 (1985), 676.*
[3] *R. J. Klein Wassink, Soldering in Electronics, 2nd Ed., Electrochemical Publications Ltd., Ayr, Scottland (1989), pp 164–166.*

of 133.3 Hz, which corresponds to typical measured readings. The increased and decreased power inputs were 1.8832 and 1.5408 W, respectively. In each load case, the duration of the pulse was 30 ms and the diameter of the laser spot was given as 0.5 mm, centered on the axis of the cylinder. The power input was assumed to be uniform across the irradiated spot.

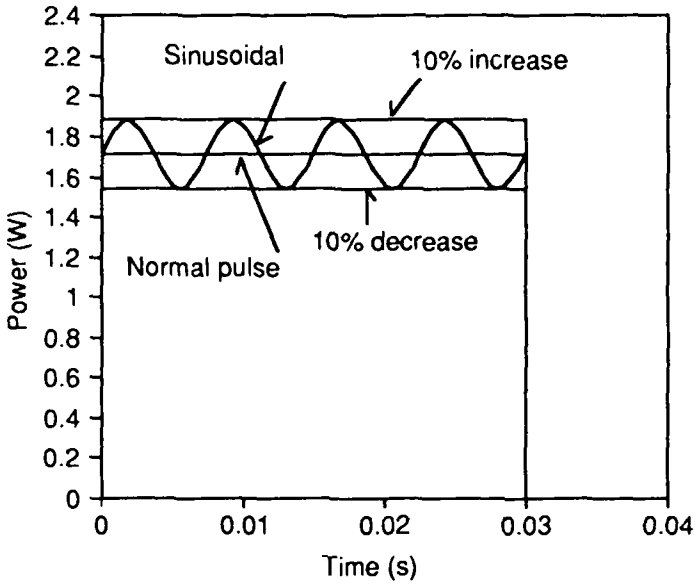

Figure 2. Laser power input for finite-element analysis load cases.

4. Results

Temperature versus time plots for a point in the center of the irradiated spot are shown in figures 3 and 4. The temperatures show an expected parabolic rise with time during the heating phase, with a maximum temperature rise of 66.8°C for the normal pulse. This compares with information from Vanzetti that the maximum temperature rise is typically in the neighborhood of 50°C. When the power input stops, the temperature drops dramatically and then stabilizes to a slow decline. This is explained by continuation of conduction away from the irradiated spot until the sample reaches an equalized temperature, approximately 70 ms after the laser terminates.

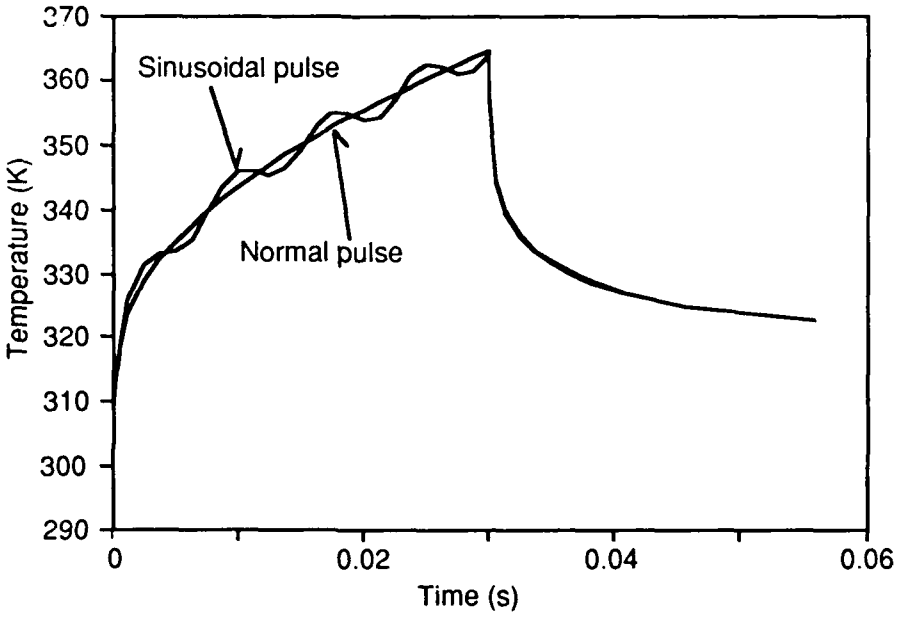

Figure 3. Finite-element analysis temperature plots for sinusoidal and normal power pulses.

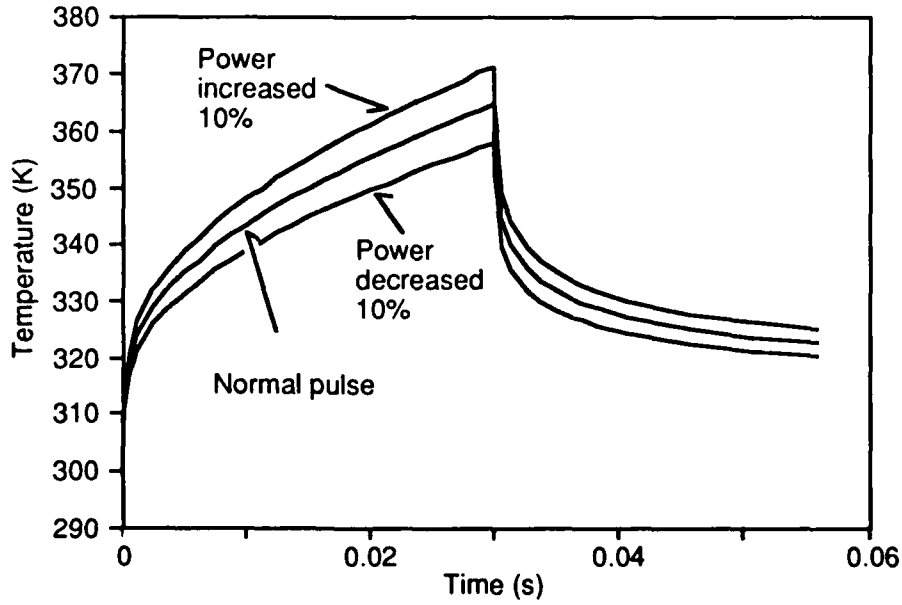

Figure 4. Temperature plots for increased, decreased, and normal power pulses.

A check of the validity of the total heat transfer is made by applying the first law of thermodynamics:

$$E_{in} = E_{stored} + E_{out} , \tag{2}$$

where E_{in} is the energy input from the laser, E_{stored} is determined from the bulk temperature increase, and E_{out} is the loss due to radiation and natural convection. Equation (2) can then be written as

$$Pt_1 = \rho VC(T_B - T_i) + hA\left(\bar{T} - T_a\right)t_2 + \varepsilon\sigma A\left(\bar{T}^4 - T_a^4\right)t_2 , \tag{3}$$

where

P = laser power,
t_1 = time of laser pulse,
ρ = density of solder,
V = solder volume,
C = specific heat of solder,
T_B = bulk temperature after stabilization,
T_i = initial temperature,
h = film coefficients on upper and lower surfaces,
A = area of exposed surfaces,
$\bar{T}$ = average temperatures on upper and lower surfaces,
T_a = ambient temperature,
σ = Stefan-Boltzmann constant, and
t_2 = time to E_{stored} calculation.

$\bar{T}$ is an averaged value; the actual surface temperature varies across the radius and in time, and an exact calculation of the E_{out} terms would require integration. However, these terms are negligible compared to E_{stored}, and the $\bar{T}$ value is sufficient for an estimation. Inserting values for the normal power pulse gives the following result:

$$\underbrace{5.136 \times 10^{-2}\ \text{J}}_{\text{Energy input}} = \underbrace{5.1322 \times 10^{-2}\ \text{J}}_{\text{Energy stored}} + \underbrace{4.003 \times 10^{-5}\ \text{J}}_{\text{Convection loss}} + \underbrace{9.457 \times 10^{-7}\ \text{J}}_{\text{Radiation loss}} .$$

This shows that the energy transfer is accurate to approximately 0.0058 percent. It also shows that the energy lost due to convection and radiation is only about 0.08 percent of the total energy and could have been omitted from the whole analysis.

The infrared emissions versus time plots, shown in figures 5 and 6, have essentially the same form as the temperature plots. The values were found using a modification of the Stefan-Boltzmann equation to account for infrared emissions only:

$$q_{ir} = \varepsilon\sigma \int (T^{2.8} - T_a^{2.8})\, dA , \tag{4}$$

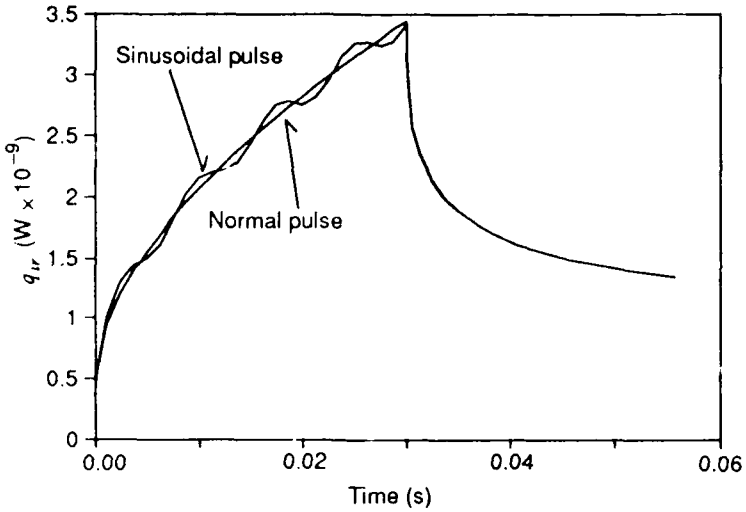

Figure 5. Infrared emission for sinusoidal and normal power pulses.

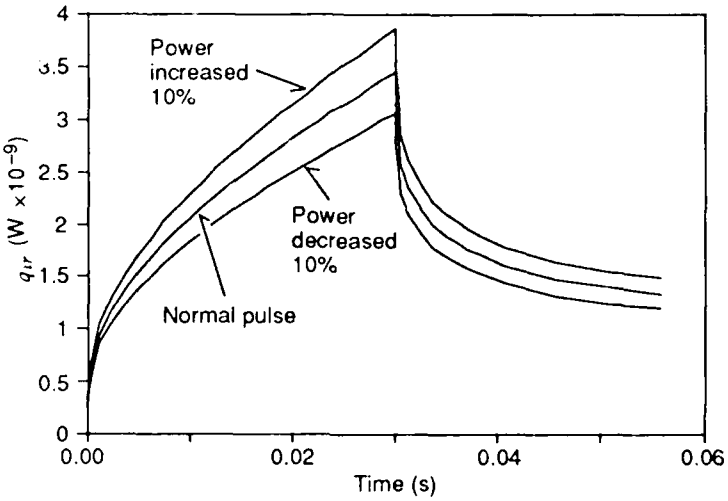

Figure 6. Infrared emission for increased, decreased, and normal power pulses.

where T is the surface temperature, T_a is the ambient temperature, and A is the area of the irradiated spot which is focused by the infrared detector. It was necessary to integrate over the area because the temperature varied significantly across the spot. The temperature was determined as a function of the radius, and was approximated as linear. The integration led to the following expression for the infrared emission:

$$q_{ir} = \varepsilon\sigma\left(\frac{2.5\times10^{-4}}{T_L - T_u}\right)^2 2\pi\left[\frac{T^{4.8}}{4.8} - \frac{T^{3.8}T_u}{3.8} - \frac{T^2T_a^{2.8}}{2} + TT_a^{2.8}T_u\right]_{T_u}^{T_L}, \qquad (5)$$

where

T_u = temperature at the center of the spot,
T_L = temperature at the edge of the spot.

In this expression, values of T_u and T_L were inserted at discrete points in time to give $q_{ir} = f(t)$, which gave the data for figures 5 and 6.

To compare the separate load cases, plots of percentage variation in infrared emissions from the normal power input's emissions were generated (fig. 7). It is seen that the sinusoidal pulse's emission varies with the power input during the heating phase, but when the power is terminated the percentage deviation from normal power quickly diminishes, with 1-percent difference immediately after power cutoff and 0-percent difference 10 ms later. The 10-percent increased and decreased power pulses' emissions, on the other hand, maintain deviations from the standard pulse of between 10 and 12 percent throughout the heating and temperature-equalizing phase.

To corroborate this last result, a mathematical expression for output error as a function of input error was derived. Since radiation and convection heat transfer are negligible over the temperature and time ranges considered, a conduction equation of the following form could be used to determine the temperature in time caused by a heat input:[4]

$$T = \frac{2q_{in}(kt)^{1/2}}{K}\left\{\text{ierfc}\left[\frac{z}{2(kt)^{1/2}}\right] - \text{ierfc}\left[\frac{(z^2 + a^2)^{1/2}}{2(kt)^{1/2}}\right]\right\} + T_i . \quad (6)$$

For our purposes equation (6) can be simplified to

$$T = q_{in} f(t) + T_i \quad (7)$$

where

T = temperature at any given time,
q_{in} = laser input power,
$f(t)$ = some function of time, and
T_i = initial temperature.

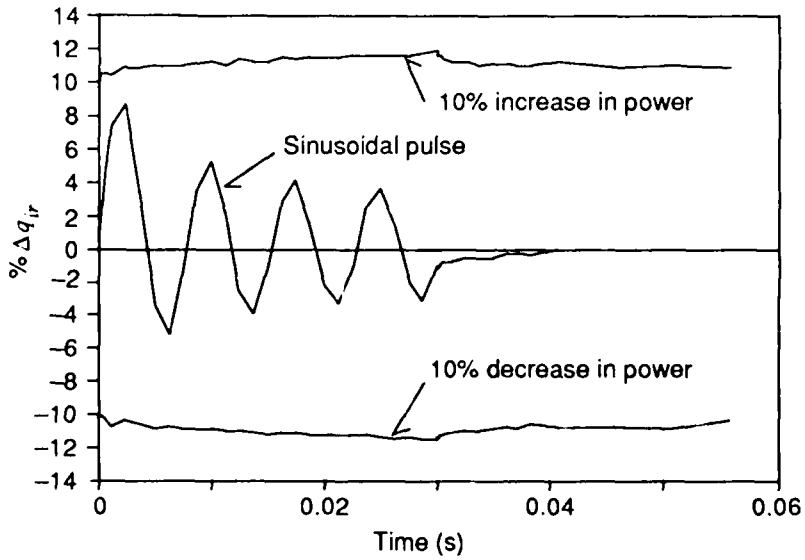

Figure 7. Percentage difference in infrared emissions from normal power pulse.

[4]*H. S. Carslaw and J. C. Jaegar, Conduction of Heat in Solids, 2nd Ed., Oxford University Press, London (1959), 2-2.*

Then for specific power inputs

$$T_1 = (q_{in})_1 f(t) + T_i, \tag{8}$$

$$T_2 = (q_{in})_2 f(t) + T_i. \tag{9}$$

Letting $(q_{in})_2 = (1 + x)(q_{in})_1$, an $(x \times 100)$-percent increase in power, all else being equal, dividing the second equation by the first, and solving for T gives

$$T_2 = (1 + x)T_1 - (x)T_i. \tag{10}$$

The percentage difference in IR emissions is found by applying the modified Stefan-Boltzmann equation:

$$\%\Delta q_{ir} = \frac{\varepsilon\sigma A\left(T_2^{2.8} - T_a^{2.8}\right) - \varepsilon\sigma A\left(T_1^{2.8} - T_a\right)^{2.8}}{\varepsilon\sigma A\left(T_1^{2.8} - T_a^{2.8}\right)} \times 100\ \%. \tag{11}$$

Inserting the $T_2 = f(T_1)$ relation gives

$$\%\Delta q_{ir} = \frac{\left[(1 + x)T_1 - xT_i\right]^{2.8} - T_1^{2.8}}{T_1^{2.8} - T_a^{2.8}}. \tag{12}$$

Predictions of errors caused by 10-, 20-, and 30-percent deviations in input power were found by setting $T_i = T_a = 298$ K, and allowing T_1 to vary from 298+ K to 370 K; these predictions are given in table 1. It is seen that the prediction of error due to a 10-percent power input deviation agrees closely with that from the finite-element analysis. Care must be taken in using equation (12), however, which requires that convection and radiation terms have a negligible effect.

Table 1. Error predictions of IR emissions

Deviation in power input (%)	Range of error in IR emission (%)
10	10 to 12.2
20	20 to 24.8
30	30 to 37.9

5. Conclusions

The results of primary interest in this study are the percentage deviation of infrared emissions from the standard pulse (fig. 7 and table 1). It is seen that 20-percent modulation about an average power will have negligible effect on the readings of the machine (less than 1-percent error), as long as the readings are taken after the laser is turned off. If readings are taken while the laser is on, errors in infrared emissions can be expected to be as high as the peak percentage input error. Also, power fluctuations that cause a net increase or decrease in power input will propagate errors in infrared emissions slightly larger than the percentage input error, with 10-percent deviations in input power leading to between 10- and 12-percent errors in infrared emissions.

Finally, the results obtained here are based on a simple model with theoretical fluctuations in input power, and are presented only to show trends. To identify possible errors in readings of a given machine, the statistical error of the machine's laser should be determined and used, and the specific sample being evaluated should be modeled more accurately.

Distribution

Administrator
Defense Technical Information Center
Attn DTIC-DDA (2 copies)
Cameron Station, Bulding 5
Alexandria, VA 22304-6145

Commander
US Army Armament, Munitions, & Chemical Command
Attn AMSMC-LEP-L, Technical Library
Attn AMSMC-ASF, Fuze & Munitions
Rock Island, IL 61299

Director
US Army Ballistic Research Laboratory
Attn SLCBR-DD-T (STINFO)
Aberdeen Proving Ground, MD 21005

US Army Electronics Technology & Devices Laboratory
Attn SLCET-DDFT
Monmouth, NJ 07703

Director
US Army Materiel Systems Analysis Activity
Attn AMXSY-M
Aberdeen Proving Ground, MD 21005

Reliability Analysis Center
RADC (RBRAC)
Attn Data Coordinator/Govt Programs
Griffiss AFB, NY 13441

AT&T Bell Laboratory
Room 4M424
Attn D. Longo
Crawfords Corner Road
Holmdel, NJ 07733

Engineering Societies Library
Attn Acquisitions Department
345 East 47th Street
New York, NY 10017

Department of Commerce
National Bureau of Standards
Attn Library
Washington, DC 20234

Director
Defense Communications Engineering Center
Attn Technical Library
1860 Wiehle Ave
Reston, VA 22090

Chief
Field Command
Defense Nuclear Agency
Livermore Division
Attn FCPRL
PO Box 808
Livermore, CA 94550

Commander
US Army Armament, Munitions, & Chemical Command (AMCCOM)
US Army Armament Research & Development Center
Attn AMSMC-TS, Technical Support Div
Attn AMSMC-QA, Prod. Assurance Directorate
Dover, NJ 07801-5001

Director
EW/RWSTA
Attn AMSEL-RD-EW-SM, EW Systems Mgt Office
Attn AMSEL-RD-EW-C, Comm Intel/Cm Div
Attn AMSEL-RD-EW-E, Elct Intel/Cm Div
Attn AMSEL-RD-EW-V, EM Vuln & ECCM Div
FT Monmouth, NJ 07703

Commander
US Army Materials Technology Laboratory
Attn SLCMT-TL, Technical Library
Watertown, MA 02172-0001

Commander
US Army Missile Command
Attn AMSMI-Q, Product Assurance
Redstone Arsenal, AL 35898-5000

Commander
US Army Natick Res & Dev Command
Natick Development Center
Attn STRNC-ML, Technical Library
Natick, MA 01760

Distribution (cont'd)

Director
US Army Signals Warfare Center
Attn AMSEL-RD-SW-RA, Analysis & Applications Div
Attn AMSEL-RD-SW-CE, Communications/ EW Division
Attn AMSEL-RD-SW-EE, Electronics/EW Division
Attn AMSEL-RD-SW-GD, General Support Systems Division
Attn AMSEL-RD-SW-OS, Office of the Scientific Advisor
Attn AMSEL-RD-SW-CAC, Project Manager—Control & Analysis Centers Office
Attn AMSEL-RD-SW-M, Resource Division Management & Plans
Attn AMSEL-RD-SW-SS, Signal Security Office
Attn AMSEL-RD-SW-DT, Tactical Data Systems
Vint Hill Farms Station
Warrenton, VA 22186-5000

Commander
US Army Training & Doctrine Command
Attn ATCD-DCS, Combat Development
Attn ATCD-AN, Analysis Dir
Attn ATCD-AN, Combat Sys Br
Attn ATCD-AN, Methodology Br
Attn ATCD-C, Telecom Comd & Con & Comptr Sys Dir
Attn ATCD-C, Battlefield Sys Integration Br
Attn ATCD-IE, Intel & EW Dir
Attn ATCD-IE, Electronic Warfare Br
Attn ATCD-T, Test & Eval Dir
Attn DCS, Combat Developments—ATCD
Attn Info Office—ATID
Attn Comm & Electronics—ATCE
FT Monroe, VA 23651

Commander
Naval Air Development Center
Attn Technical Library
Warminster, PA 18974

Director
Naval Research Laboratory
Attn 2600, Technical Info Div
Washington, DC 20375

Commander
Naval Surface Weapons Center
Attn DX-21 Library Div
Dahlgren, VA 22448

Commander
Naval Surface Weapons Center
Attn E-43, Technical Library
White Oak, MD 20910

Commander
Naval Telecommunications Command, HQ
Attn Technical Library
4401 Mass Ave, NW
Washington, DC 20390

Superintendent
HQ, US Air Force Academy
Attn Tech Library
USAF Academy, CO 80840

Commander
HQ, Rome Air Development Center (AFSC)
Attn Le, Deputy for Electronic Tech
Attn LMT, Telecommunications Br
Griffiss AFB, NY 13441

Commander
HQ, Air Force Systems Command
Attn Technical Library
Andrews AFB
Washington, DC 20334

Director
NASA
Attn 250, Tech Info Div
Goddard Space Flight Center
Greenbelt, MD 20771

Director
NASA
Attn Technical Library
John F. Kennedy Space Center, FL 32899

Director
NASA
Attn Technical Library
Langley Research Center
Hampton, VA 23665

Distribution (cont'd)

Director
NASA
Attn Technical Library
Lewis Research Center
Cleveland, OH 44135

Sandia Laboratories
Livermore Laboratory
PO Box 969
Livermore, CA 94550

Sandia National Laboratories
PO Box 5800
Albuquerque, NM 87185

US Army Laboratory Command
Attn Technical Director, AMSLC-TD

Installation Support Activity
Attn Legal Office, SLCIS-CC

USAISC
Attn Record Copy, AMSLC-IM-VA
Attn Technical Reports Branch,
AMSLC-IM-VP (2 copies)

Harry Diamond Laboratories
Attn Division Directors
Attn Library, SLCHD-TL (3 copies)
Attn Library, SLCHD-TL (Woodbridge)
Attn Chief, SLCHD-NW-CS
Attn Chief, SLCHD-NW-E
Attn Chief, SLCHD-NW-EH
Attn Chief, SLCHD-NW-EP
Attn Chief, SLCHD-NW-ES
Attn Chief, SLCHD-NW-P
Attn Chief, SLCHD-NW-R
Attn Chief, SLCHD-NW-RP
Attn Chief, SLCHD-NW-RS
Attn Chief, SLCHD-NW-TN
Attn Chief, SLCHD-NW-TS
Attn T. Bayba, SLCHD-TS-PR (5 copies)